# Equatorial Radar Array for Detection and Characterization of Earth-Orbiting Objects

**Ms. Kathleen Minear & Dr. G. Patrick Martin**
*Specialized Arrays Inc.*

## ABSTRACT

A comprehensive solution for detection and one-pass accurate characterization of Earth-propagating objects that incorporates widely-spaced coherent transmit arraying has been developed, modeled and simulated. Performance characteristics, enabling technologies, how it works and future direction will be presented.

The widely-spaced Equatorial Space Situational Awareness Radar (ESSAR) works on the principal that ALL propagating (non-station-kept) Earth-orbiting objects will pass through a strategically placed array beam and with advanced hardware and algorithms those objects can be accurately characterized immediately. The object's orbital parameters are determined within a single pass coincident with its detection.

On a two-year government contract ending on September 29, 2010, we led a team of engineers in a successful demonstration of widely-spaced large reflector coherent transmit arraying at X-band to the DSCS B13 satellite. The system consisted of three 12m reflectors set more than 60m apart (>2000 wavelengths). This break-through capability is one of the enabling technologies.

In this demonstration modulated signals from the three 12m antennas were combined at 8GHz with nearly theoretical results. During a Florida tropical depression less than 0.3 dB combining loss was achieved. Critical advances from this demonstration included (1) the instant availability of the array (no system calibration is required), (2) phase transfer synchronization (vs. time), (3) complex envelope beamforming at baseband and (4) real-time atmospheric compensation. Because of these features it was recognized by NASA to be the first operationally feasible solution for widely-spaced, large reflector, coherent transmit arraying.

Over the last six years we have developed a method and system for SSA using a radar array of widely-spaced ground reflectors. The enabling technologies are: (1) location near or on the Equator and orientation pointing towards the horizon, (2) very high precision AOA (3) specialized hardware for time differentials and Doppler, (4) specialized algorithms for target location and velocity determination and (5) widely-spaced coherent transmit arraying (providing exceptional EIRP, G/T and AOA). From these measurements we calculate orbit parameters. Importantly, this method mitigates the too short arc (TSA) problem, (object time in the beam) due to the high precision AOA resulting from the array diameter, orientation and advanced algorithms.

Preliminary simulations show that with only a three reflector minimal configuration, -40dBsm (marble sized) objects can be detected up to 1000km with orbital element parameter errors of tens of meters positional and a few cm/sec velocity. Importantly the array can immediately transition to an ISAR imaging mode while the system tracks the object. The widely-spaced radar array is expandable for smaller objects and longer distances.

## 1. INTRODUCTION

This paper presents a method and notional system design for Space Situational Awareness, SSA using a radar array of widely-spaced ground reflectors, Fig 1. By virtue of its location (near or on the Equator), orientation (pointing towards the horizon), advanced arraying technology, waveform and algorithms, the Equatorial SSA Radar (ESSAR) has the potential to comprehensively detect and within only one-pass accurately determine the orbital elements of Earth-propagating objects[1] including orbital debris [1].

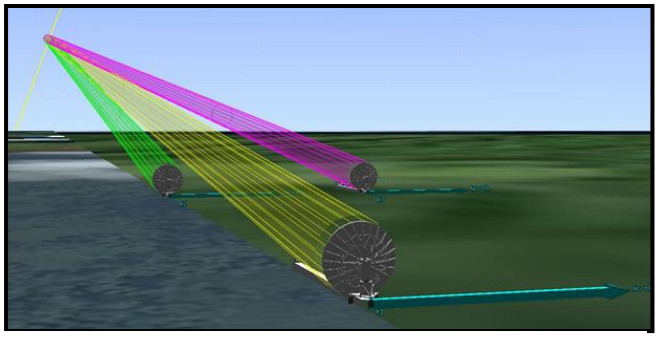

Fig 1 Notional Equatorial SSA Radar, ESSAR

[1] Marble-sized LEO objects with a minimal three antenna system; expandable for extended range or smaller object cross section

ESSAR could potentially complement Space Fence. While Space Fence instantaneously detects objects passing through its field of view, ESSAR comprehensively detects persistent Earth-propagating objects; most in a few months.

Since an object's orbit can be determined during the pass, the array can immediately transition to an ISAR imaging mode while the system tracks the object. Low observable objects may be more detectable due to the high sensitivity, unique perspective and wide bandwidth waveform.

An array of large ground reflectors can produce exceptionally high EIRP and G/T, contributing to high sensitivity. A wide bandwidth waveform provides precise range/range-rate, and the wide aperture spacing provides excellent AOA (Angle of Arrival), in turn leading to precise cross range and velocity. As an enhancement option, near-equator low complexity multi-static stations can provide detection and orbit determination from a single pulse within a pass.

As an example, a notional minimal system could be composed of three 12m reflectors located about 60m apart on a scalene triangle. A 10GHz frequency of operation and system bandwidth of 100MHz will support < 3m range and < 1.5m/sec range rate. With 1KW HPA's, the array can produce nearly 100dBW EIRP, and about 46dBK receive G/T with uncooled preamps, supporting single pulse SNR of 10dB for a -40dBsm (marble sized) object at LEO. With > 2000 $\lambda$ spacing, AOA of about 10 $\mu rad$ is expected, leading to cross-range position accuracy commensurate with range at LEO. These parameters in turn support orbit positional errors of 10's of meters and m/sec velocity.

Performance characteristics, how it works, modeling and simulation results and a future direction are presented.

## 2. PERFORMANCE CHARACTERISTICS

Advantages of ESSAR include:

- Comprehensive detection and one-pass orbit characterization of Earth-propagating objects[2] including
    - Assets in LEO/MEO/HEO
    - Orbital debris
    - Unknown entities including co-orbital systems[2]
- Wide field-of-view for object detection (that of a single element's beamwidth vs the array beamwidth)
- High object resolving power determined by the array beamwidth (vs that of a single element)
- 24/7/365 availability; day/night/cloudy/clear operation
- Unique coverage of LILO objects missed by other systems
- Comparatively low cost, $10's of millions vs $100's of millions
- Staring sensor (or single plane scan for special cases)
- Unusual perspective gives up to 81 times longer view than overhead
- Unusual perspective may provide better detection of LO
- Wideband long duration waveform circumventing active avoidance
- One-encounter orbit determination (two or more observations within most encounters)
- Ability to immediately transition to tracking/ISAR imaging
- Array scalability for extended range or smaller object cross section
- Much simpler CONOPS compared with scanning approaches
- Multi-static options (one Tx and multiple Rx stations) can get a precise orbit in one pulse vs one pass
- Alternate modes address Geo-stationary and Geo-synchronous objects

Additionally it is able to detect and characterize objects missed by other systems such as low inclination low orbit (LILO) objects. Station-kept (vs Earth-propagating) objects can be handled using three world-wide systems and single plane scan mode.

A notional design uses 12m reflectors which are a commodity versus expensive custom antennas. InterTronic Solutions' 12m antennas were used in our prototype coherent transmit demonstration on NASA's Transmit Adaptive

[2] ibid

Combining Experiment, TxACE program (2008- 2010). Enhancements have been incorporated in their antenna design for ease of arraying.

This technology differs from traditional radar arrays in that coherent transmit from widely-spaced sensors is an inherent feature versus one location transmitting and multiple receiving. The array creates a smaller beam on the object and thus higher resolution AOA as well as enabling higher system sensitivity and operational flexibility. Note that the sensors could be phased arrays themselves; this technology is not limited to reflector antennas.

## 3. ENABLING TECHNOLOGIES

ESSAR enabling technologies:

1. Location near or on the Equator and orientation pointing towards the horizon
2. Very high precision AOA
3. Specialized hardware for time differentials and Doppler
4. Specialized algorithms for target location and velocity determination
5. Widely-spaced coherent transmit arraying methods

A critical enabling technology is that the proposed widely-spaced radar array is location on or near the Equator and its orientation pointing towards the horizon. It is worth noting that use of an array is attractive because of the $N^3$ dependence on the number (N) of antenna elements (and precise wide baseline AOA potential). Transmit array gain increases by N, then since each antenna is also individually powered, total power transmitted increases by N as well, and finally, receive array gain is proportional to N, thus the $N^3$ dependence (if transmit and receive arrays have equal number of dishes, otherwise $N_{Tx}^2 * N_{Rx}$)). These advantages are in addition to the usual array benefits such as graceful degradation with failure, and dynamic re-configurability.

### 3.1 Location near or on the Equator and orientation pointing towards the horizon

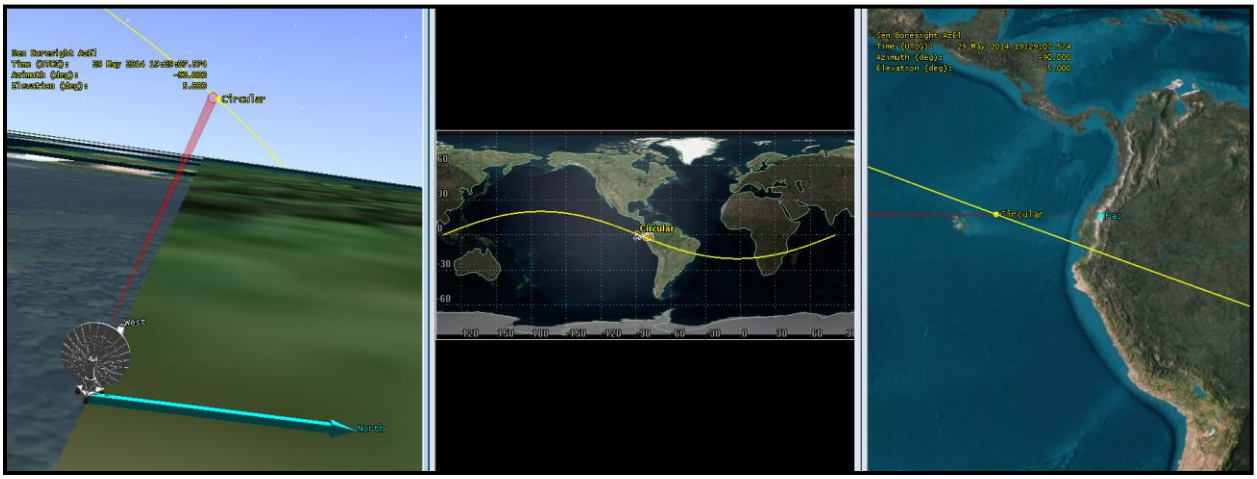


Fig 2 Evaluation of access to orbits using STK

The proposed system works on the principal that ALL propagating (non-station-kept) Earth-orbiting objects will pass through a strategically placed array beam and with advanced hardware and algorithms those objects can be characterized with unprecedented accuracy immediately.

A preliminary evaluation of object access time in the antenna beam was conducted using System Toolkit, STK[3], as illustrated in Fig 2. A single reflector was modeled since that corresponds to the array's element beamwidth. The antenna is located on the equator (in Ecuador), pointed 5° above the horizon, a practical step to keep near sidelobes off the hot earth. Thousands of random orbits were evaluated with altitudes up to 20000 km and inclinations up to

[3] Analytical Graphic, AGI's System Toolkit, STK

20°. The plots depict the total time an object was in the beam over a year as a function of object altitude (y-axis) and object inclination (x-axis). This analysis was repeated for an array location at 7° latitude with the antenna pointing to zenith. The results clearly show the benefit of placing the SSA radar array near or on the Equator.

Results are given in Fig 3 for the proposed approach, 0° latitude pointing at 5° elevation and in Fig 4 for a system at 7° latitude pointing straight up, with object altitude on the ordinate and inclination on the abscissa. Colors depict access time, with red best (clamped at 80 minutes/year) and blue good, with dark blue 10 minutes/year. Black depicts zero access during this time period. The y-axis is the object altitude (0-20,000km for this run). The x-axis is the object inclination (0-20° for this run). Note the lack of low-inclination low-orbit object access (black area).

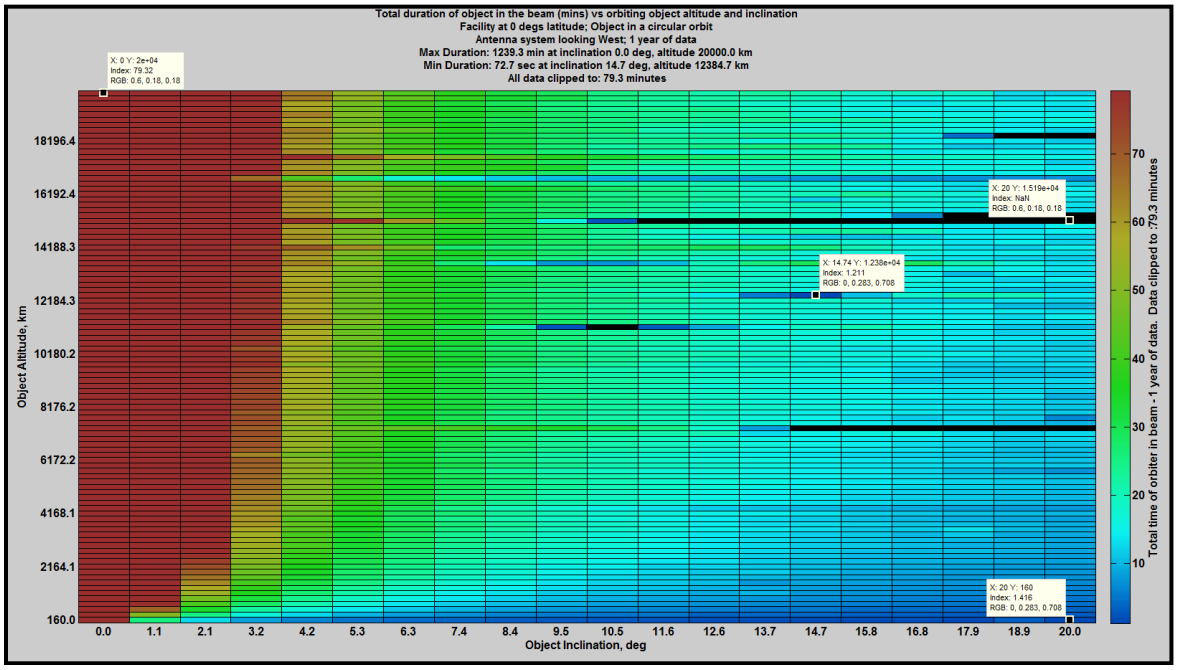


Fig 3 Total access time to targets during one year for ESSAR located at 0° latitude and pointing at 5° elevation

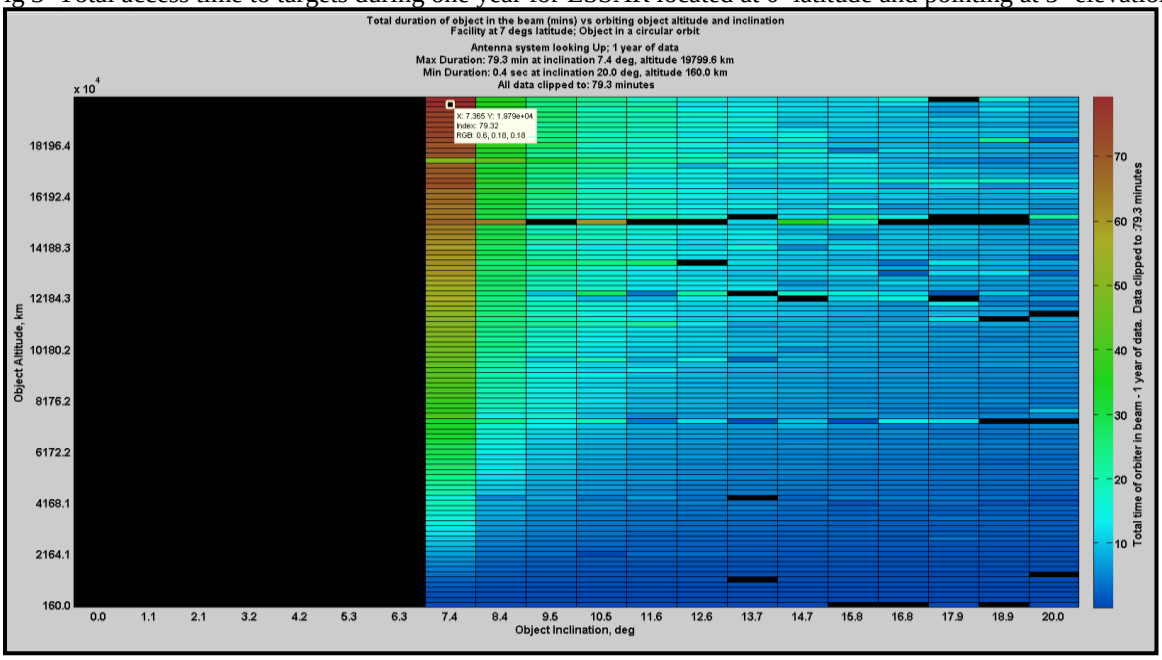


Fig 4 Total access time to targets during one year for a system located at 7° latitude and pointing at 90° elevation

Low elevation staring in equatorial plane provides a much longer observation time vs overhead Fig 5. Even fast polar LEO objects are in the beam long enough for reflecting multiple pulses

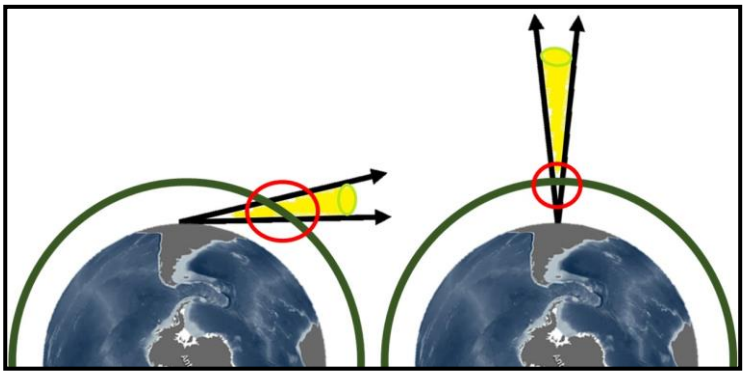

Fig 5 Low elevation staring intercepts objects (note green trajectory) at greater range resulting in a much bigger spot size (at left) than overhead (right).

The polar view in Fig 6 illustrates how targets are accessed. The earth is viewed with North Pole in the center as seen from above. An array is located on the equator; depicted as a red ellipse. Reflector antennas in the array are pointed westward just above the horizon. Two objects are shown crossing the equatorial plane in LEO and MEO prograde orbits. The beam may also be traversed from north to south (or vice versa) due to orbital inclination; target motion may be prograde or retrograde. The LEO object is depicted in a circular orbit with altitude H above the surface. This object experiences a prolonged duration within the conical beam due to its slanted orbital path through the beam.

Such arrangement of the array beam on the horizon gives about nine times more coverage time to the faster moving LEO object than available with an overhead view and at the same time minimizes the radar range variation from closest to most distant object. This helps with maximizing duty cycle (set by round trip differential delay) and reducing dynamic range. Importantly, beam area for detecting LEO objects is about 81 times larger at the slant range than overhead, greatly improving the probability of detection and mitigating the TSA problem and about 10 times longer view for LEO polar than overhead starting. Higher altitude objects are in the beam longer, permitting longer observation time.

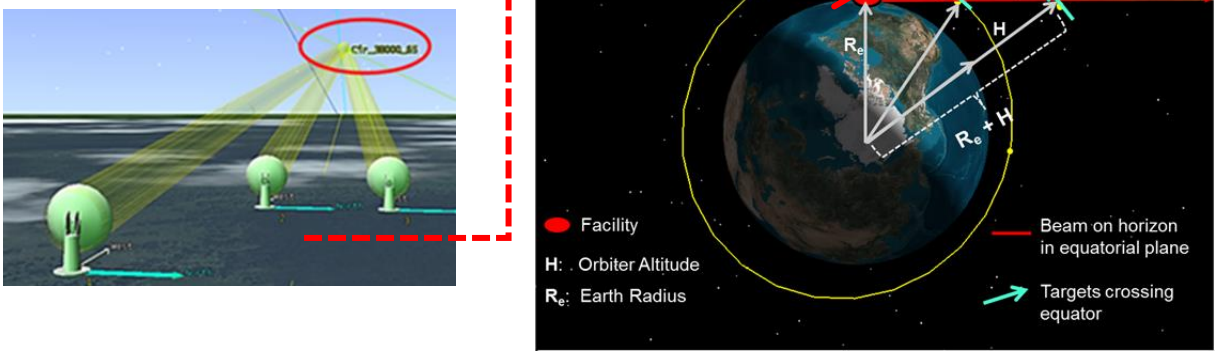


Fig 6 Low elevation staring provides longer viewing time compared with overhead pointing

### 3.2 Very high precision AOA

Our array Angle of Arrival, AOA method determines the relative azimuth and elevation angles to a received signal source from array boresight. Fundamentally, this utilizes the wide spacing of the reflectors in wavelengths, providing excellent angular resolution.

When a target return signal is detected, buffered array receive data are processed to extract the steering vector associated with the return '$SV_R$'. A function generated from $SV_R$ is correlated with the array calibration manifold; call it 'Q', (via covariance of de-spread signals from the array elements). AOA is estimated by finding the calibration

vector that most nearly matches the measured steering vector. The minimum correlation corresponding to the best AOA estimate is depicted in Fig 7 where the x and y-axis are azimuth and elevation angles and the z-axis is 'Q'.

Our method uses an orthogonal root-finding process that includes accommodation for arbitrary polarization, with the best Az/EL determined by the best null. This process inherently develops a confidence factor related to the null depth, so that AOA estimates (and thus position estimate errors) can be optimally weighted in the orbit determination process.

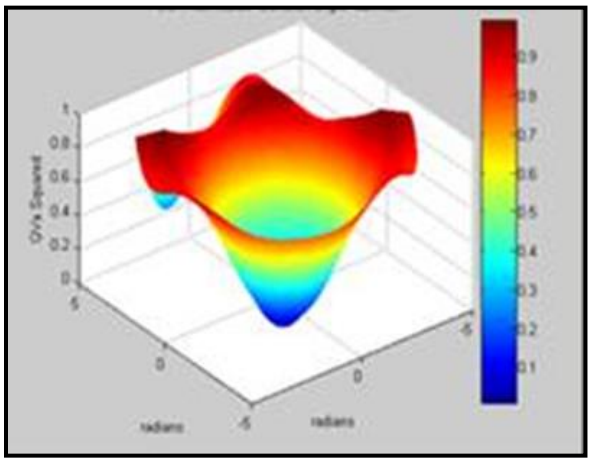


Fig 7 AOA determined with calibration manifold and 'SVR'

The calibration manifold is precisely maintained operationally by our array-wide closed-loop phase control process, from reflector surface to array output, similar to the transmit closed loop control process. This ensures that no calibration drift occurs. Our closed-loop phase control process is discussed in depth [3, 4].

Since the antennas are widely spaced, highly accurate AOA is realizable; typically better than 1/50 of the array beamwidth. Obviously, wide element spacing results in a multitude of grating lobes. In a uniform array of identical elements identically oriented, this would result in perfectly ambiguous angles. We developed and tested an effective mitigation solution. These (and other) techniques cause what would have been ambiguous peaks to be clearly distinguishable.

Both AOA calibration and high precision open-loop transmit beamforming require that

- All RF circuits are under closed-loop phase control (including LNA, HPA, filters, etc.). Consequently, circuit contributions to the calibration error budget can be made negligible

- All antenna radiation effects are addressed using model-based predictions, photogrammetry and ARP (Antenna Reference Point) surveys, and continually measured antenna orientations

Using measured range to a target, cross-range is obtainable through AOA. In principle, cross-velocity can be calculated by using the differences between multiple-pulse position determinations, "delta position/delta time". At least two pulse measurements are required. For our simulations all of the individual direct measurements (range, range-rate and AOA) were input to Analytical Graphics Orbit Determining Tool Kit (ODTK), which optimally weights and combines these individual measurements to obtain orbital elements.

### 3.3 Specialized hardware for time differential and Doppler frequency

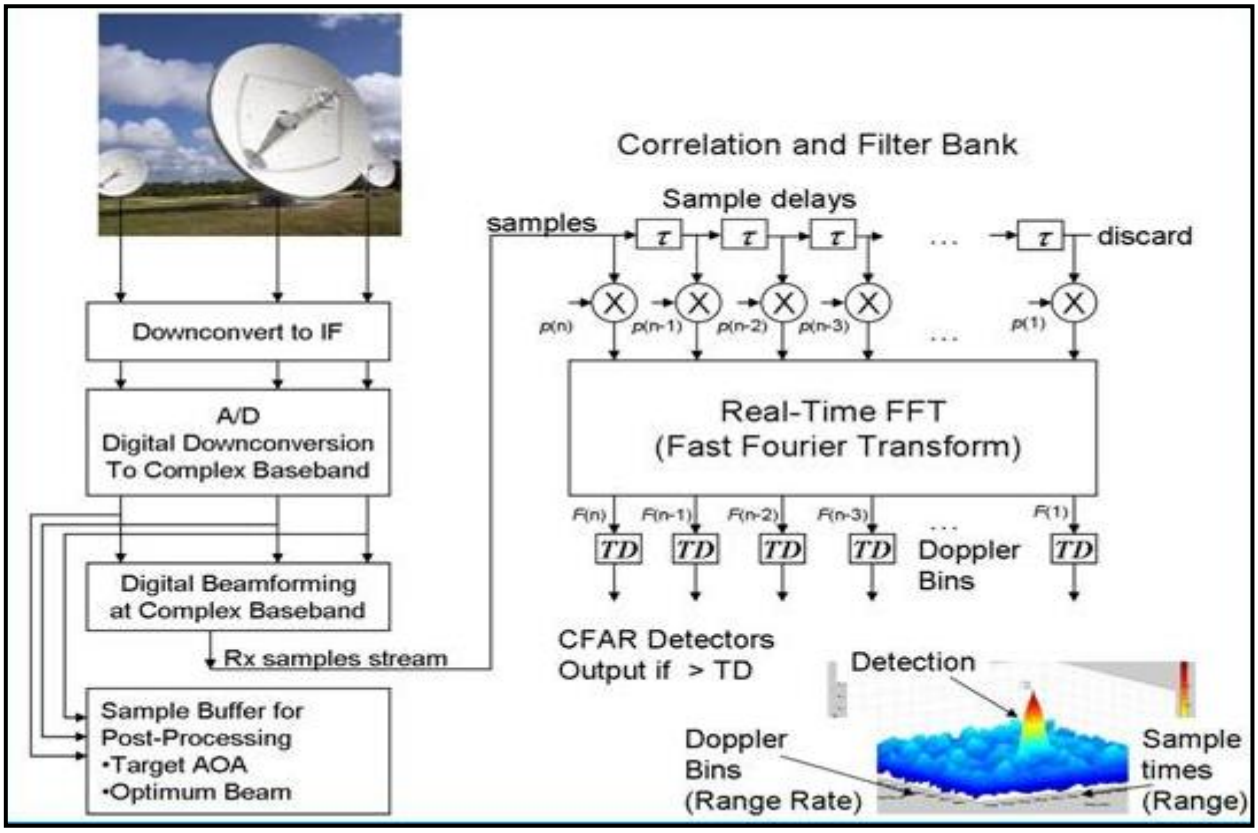


Fig 8 Notional radar receive signal processing flow

A binary PSK pseudo random sequence waveform is selected vs. chirp since range and range rate are decoupled, and with non-repeating PN, potential range ambiguity is eliminated. In Fig 6, the transmit pulse lasts until a return is expected from the nearest LEO object (160km), in this example just under 10ms. The array then receives until a return can arrive from the furthest MEO object (1000km), about 25ms. Thus, the cycle period is about 35ms and the duty cycle is about 1/3. (Keep in mind with reference to Fig 6, that we must consider slant range, not target altitude). A transmit frequency of 10GHz and a chip rate of 100Mc/sec will give a raw range resolution of less than 3m, and range rate resolution of $\approx 1.5 m/s$ via Doppler. Signals from the antennas are coherently downconverted to baseband, digitally sampled at greater than the Nyquist rate then digitally weighted and combined into a default boresight beam output; see Fig 8. (In post processing, this default beam will be optimized.)

This output is passed to a transversal filter loaded with pulse PN sequence coefficients for wipe off the received bits. When alignment is obtained at a particular target's range, the multitude of taps will each output a sample of the Doppler sine wave. These are very weak narrowband signals in the presence of wideband noise, and they must be filtered and combined. A Fourier transform is a good approximation to the ideal matched filter with transversal filter taps taken as an input vector. FFT outputs are CFAR threshold detected. Simulated system output is shown for a LEO object prior to CFAR.

Two-way range to the target is obtained from the difference between pulse transmission time and CFAR output time. With the speed of light (free space and atmosphere segments aggregated), the time differential is converted to target range. Meanwhile, the CFAR bin with the detection designates the Doppler shift of the return. With carrier frequency known, the Doppler shift can be expressed in terms of range-rate.

*FFT considerations*

As discussed, the taps on a transversal filter are weighted by the transmitted PN sequence, with one tap for each bit. As received samples flow through the tapped delay line, eventually samples from a received echo align with the PN coefficients. This alignment persists for one sample time. At the moment of alignment, the PN bits are 'wiped off', revealing a sampled, Doppler shifted sine wave, persisting for only one sample duration. With the example system parameters, a target at the threshold of detection would result in this Doppler shifted sine wave having a SNR of about -50dB. After the FFT, the appropriate Doppler tap would have a sample duration output of about 10dB.
The example design used a carrier frequency of 10GHz, a PN bit rate of 100Mbps, and a pulse duration of 10ms; thus about 1,000,000 bits in duration. This means that the transversal filter must have one million taps and that processing to detect the weak sine wave must reoccur every 10ns.

Our idealized choice to realize this processing is the FFT, but this is infeasible with current technology. However, the required processing is not as impossible as it might at first appear. In this application, only a few simultaneous targets, probably only one or two are expected. This means that a sparse frequency domain environment is present. Great simplification in the FFT is possible under such sparse conditions (SFFT). Even further, a major simplification of the required FFT by more than two orders of magnitude may be possible in this application. For the example design parameters and a carrier frequency of 10GHz, the maximum Doppler shift possible will be about 540KHz (LILO object). A general FFT of one million points processing a 100MHz signal will have one million outputs, separated in frequency by 100Hz each. This means that only 5,400 outputs of the one million possible will ever be needed, a potential simplification of 185 times.

In terms of existing hardware, MIT Lincoln Labs has produced a one million-point FFT ASIC producing outputs every 10ms. They expect the next ASIC generation to run in 1ms or less. ASICS like these could in principle be operated in parallel.

It should be noted that a less accurate yet still effective radar design could be organized around an S-band carrier frequency and a proportionately reduced waveform bandwidth, roughly a factor of five in each parameter. This would in turn reduce the required FFT complexity by an additional factor of about 25, almost certainly realizable in the near term.

Both DARPA and NSF have supported SFFT work at MIT.

### 3.4 Specialized algorithms for target location and velocity determination

An object's return in a range/Doppler bin obtains two of the possible four parameters available from a monostatic radar array of this type. Since orbit determination requires six parameters, the additional cross-range values required to complete a 3D position determination are obtained using the array's AOA algorithm. With more than one returned pulse processed (typically many within a pass) cross-range position differentials can be calculated, providing cross-range velocity estimates. With an optional multi-static system extension, all six orbital parameters can be measured with a single pulse.

Received samples from each antenna are held in a short duration buffer to enable recall of the inputs that produced detection. It is pointless to compute full-bandwidth covariance matrices from the wideband inputs, since a "just detectable" signal's SNR in the full bandwidth is about -50dB. After detection, PN wipe-off timing and precise frequency for narrow band filtering is known, so useful covariance matrices can be computed. With steering vectors and system calibration, AOA is determined and with range provides cross-range position.

The pulse was initially received with the default transmit beam, and the object was not likely at the peak. Since the steering vector obtained in the AOA step as well as range and Doppler filtered inputs are now available, the signal can be optimally received via buffered data. This could provide several dB improvements overall. Dual polarization optimum beam forming could yield a nominal 3dB SNR improvement as well as provide valuable information about the object's composition. Pol inputs can be combined pre-D since we expect they will share a range/Doppler bin (or at least a Doppler bin). Dual pol transmit is highly desirable and feasible, but discussion is beyond the scope of this paper.

The object is expected to be in the beam for dozens of pulses, permitting post-detection processing improvement. Because these detections have positive SNR post-detection combining is almost as good as pre-detection combining.

SNR of post detection combining improves almost linearly with the number of samples for positive SNR samples. Consequently, given a target detectable with a single pulse we expect an improvement in effective SNR over a pass by up to 18dB. AGI's Orbit Determination Toolkit, ODTK, was used to optimally combine range, range-rate and cross range samples, yielding single pass velocity errors of about 5cm/sec for a particular simulated LILO object.

With the notional system stated previously (three 12m dishes, X-Band, 1KW air-cooled HPA's), the array will produce nearly 100dBW EIRP. We estimate a system temperature of 70K. With modest cryogenic cooling 35K is realizable. A minimum elevation of 5° helps reduce noise from the hot earth seen through sidelobes.

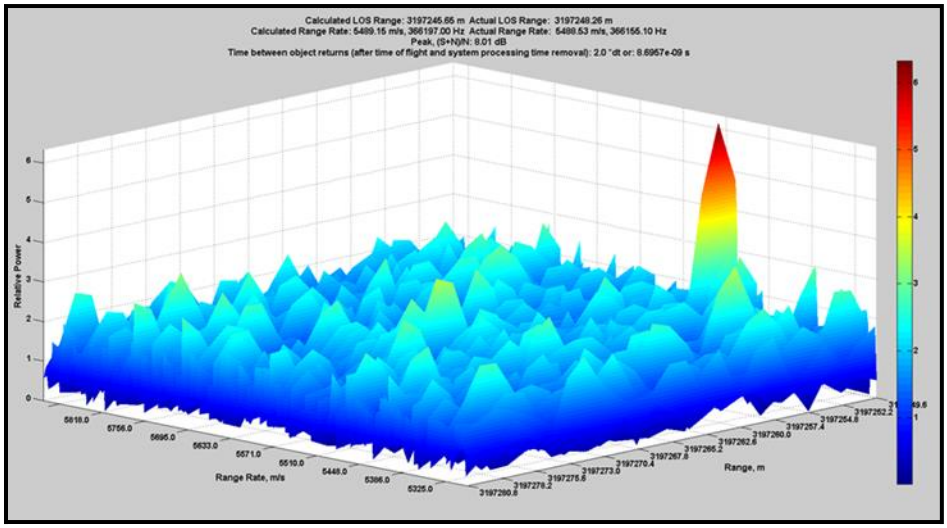


Fig 9 Object detection process from simulated FFT processor and algorithms

This supports a single pulse SNR of about 10dB for a marble sized cross section (-40dBsm) in a 160km orbit or a tennis ball sized cross section (-30dBsm) in a 1000km orbit. (Due to slant range considerations, target altitude is not the same as range).

Data from particular objects were analyzed with respect to the ability of our simulated FFT processor and algorithms to back out original orbit parameters. Resulting errors were quite small. Here we present one such case.

An object of about 7cm diameter in a circular orbit at 1000 km with an inclination of 20 degrees is considered. Each pulse that returns from the object generates a peak (power) as a function of range and range rate (Fig 9). The x-axis is range, y-axis is range rate and the z-axis is relative power with the peak = (S+N)/N = 8.01 dB. An FFT of the product of the receive signal with the transmitted PN for a series of 25 delays yields this surface. The range and range rate (x and y axis) can be derived from the result. With two measurements of range and range rate and the angles of arrival of the signal, the orbit parameters could be calculated.

A comparison of the actual LOS range and range rate from AGI's STK to the range and range rate found using our signal processing method is given in Table **1**. As the object continues through the beam, measurements were taken every 0.035s and these calculations repeated.

Table 1

| | **Range** | **Range Rate** |
|---|---|---|
| **Actual** | 3,197,248.26 | 5488.53 m/s, 366155.1 Hz |
| **Calculated** | 3,197,245.65 | 5489.15 m/s, 366197 Hz |

RMS errors for range and range rate were calculated and used in ODTK to seed the least squares, LS estimate from measurements of azimuth, elevation, range, and Doppler.

Range, Doppler, azimuth, and elevation errors were added corresponding to our methods and hardware design. Process and white noise were also added. Keplerian orbit parameters, position and velocity uncertainties were calculated using AGI's ODTK.

Next the estimate attained from LS was transferred to the object. After filtering an orbit estimate was created and updated ephemeris was output. After additional post-processing, position and velocity errors were output. Radial, in-track and cross-track position were approximately 44.5, 28.7, and 19.8 meters respectively. Radial, in-track and cross-track velocity errors were approximately 0.059, 0.039, and 0.020 meters per second respectively.

### 3.5 Widely-spaced coherent transmit arraying methods

Unlike typical SSA radar systems the antennas that transmit are very widely spaced. Due to the effective aperture being the diameter of the array rather than a single antenna, AOA resolution, thus cross-range distances formerly not realizable are now possible.

Coherent transmit from widely-spaced antennas is significantly more challenging than coherent receive arraying. For widely-spaced receive arrays the signal arrives at each sensor and can be post-processed and coherently combined. However for transmit the timing requirements were not realizable using widely-spaced antennas without expensive custom antennas and temperature controlled fiber and electronics and extraordinary calibration techniques. Even then to mitigate tropospheric phase variation the system required extensive calibration along the line of sight to the target and as the atmosphere along the path changed the system required re-calibration.

Fig 10 Array of three 12 m antennas (Martin-Minear Method)

From 2007 to 2010 NASA sponsored three coherent transmit experiments two at JPL respectively by Vilnrotter and D'Addario and one at Harris Corporation by Martin and Minear [5]. The later was considered to be operationally feasible[4] by NASA [6, 7]. The demonstration array is shown in Fig 10.

The Martin-Minear Method mitigated the three principal uplink array error contributors [3, 4].

1. Determination of time of flight phase differential
2. Autonomous continual control of all circuit phase differentials
3. Real-time mitigation of tropospheric effects

*3.5.1 Determination of time of flight phase differential*

Differential phase errors due to the time of flight from each antenna reference point to the target were mitigated using a model-based approach (Fig 11) and refined using a solution of equations constructed from tracking known satellites. If the element phase centers are surveyed to a small part of a wavelength (mm at X-Band) with respect to ENU coordinates, phase beam-steering based on an array model is feasible.

[4] "IntelArrays' (now Specialized Arrays) principals are the originators of and the only team in the world that has demonstrated operationally feasible, real-time radio frequency adaptive optics techniques."

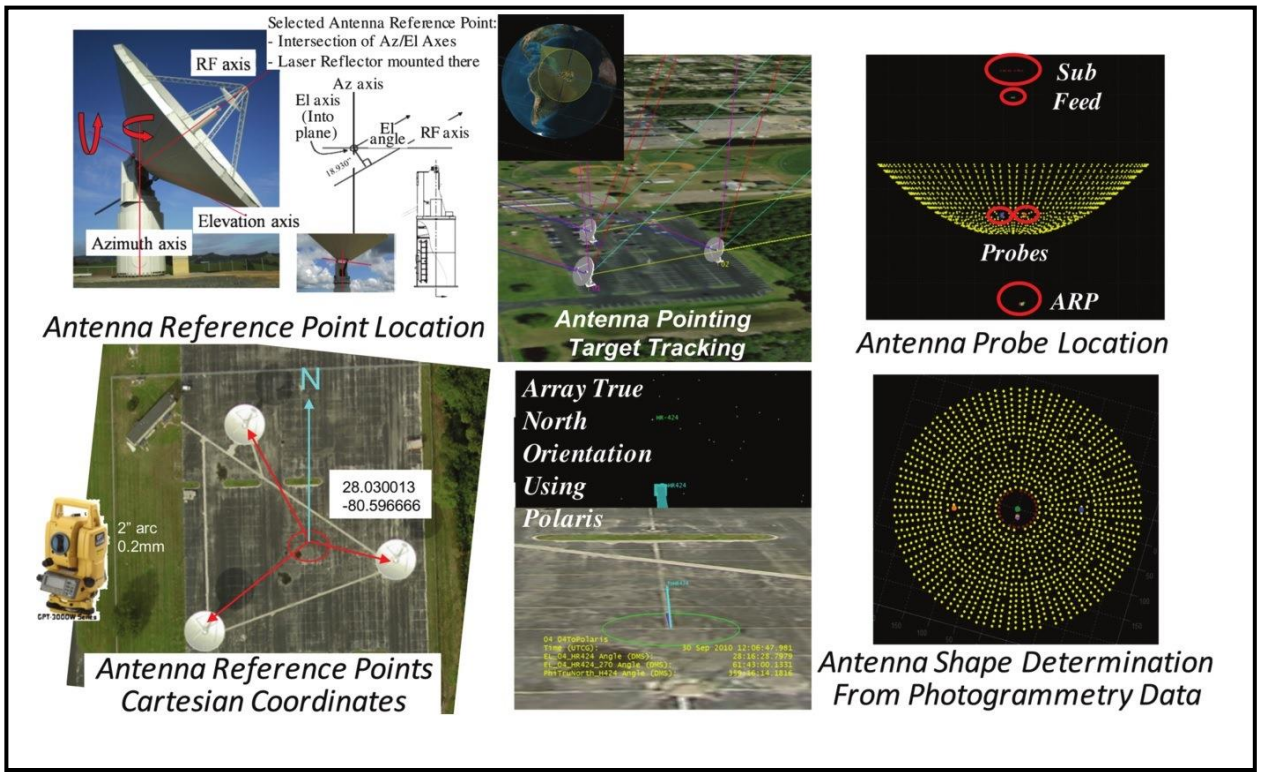


Fig 11 A model-based approach was used to find the antenna reference points and the array's orientation to true north

While this method works well for static systems an alternate approach has been developed for other applications such as on-the-move ground vehicles and very widely-spaced (kms) antennas [8].

*3.5.2 Autonomous continual control of all circuit phase differentials*

The second error contributor was the phase differential due to the circuitry. This included fiber-optic transmission links, up/down converters, filters, fiber-optic transmitters and receivers and power amplifiers. These are all temperature sensitive and time variable. Conceptually, real-time autonomous continual closed-loop circuit error correction is depicted in Fig 12.

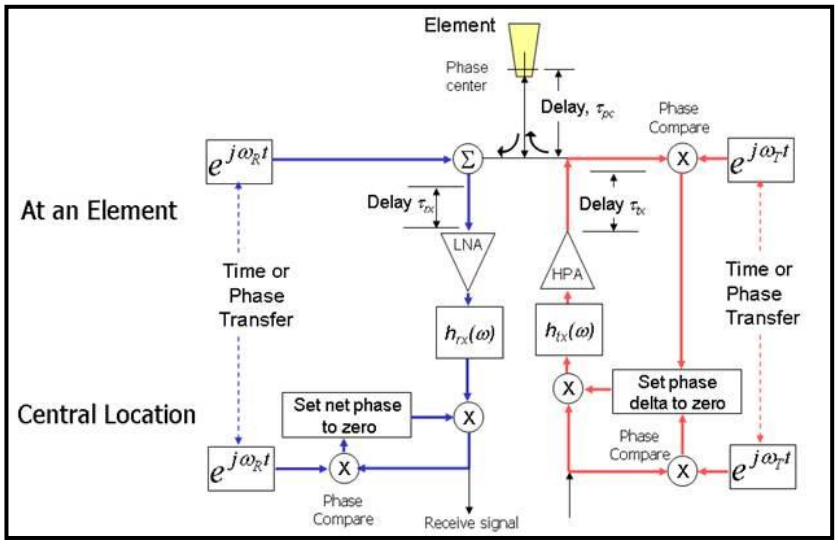


Fig 12 Conceptual depiction of phase transfer across long distances

This error contributor was solved by applying continual closed-loop phase correction from baseband signal generation through the RF signals as they leave the reflector surfaces. This was enabled by a new (at the time of the experiment) transmission paradigm, **complex envelope** (vs. precision time delay) beamforming. By independently addressing carrier phase and information alignment, all of the

transmit array circuitry can be put in a spatially distributed closed loop driving to zero phase differential. Meanwhile time delay, applied digitally in convenient sub-inverse bandwidth increments at baseband (zero frequency, so phase is not affected) independently aligns information.

We implemented phase transfer rather than time transfer (see 'Time or Phase Transfer' to the right in Fig 12). It was implemented within error detection assemblies and tested prior to installation on each antenna. Results of an 83+ hour test (phase transfer over long, variable distances) using the error detection and correction assemblies are shown in Fig 13. The phase differential between two assemblies (1000's of wavelengths apart) after correction is on the y-axis and time in seconds (3e5) on the x-axis. The error budget for this error source was 3° RMS and 10° peak; 1.4° RMS and 8° peak was achieved. After this test they were installed on the antennas behind the field sensors as seen on the right of Fig 14.

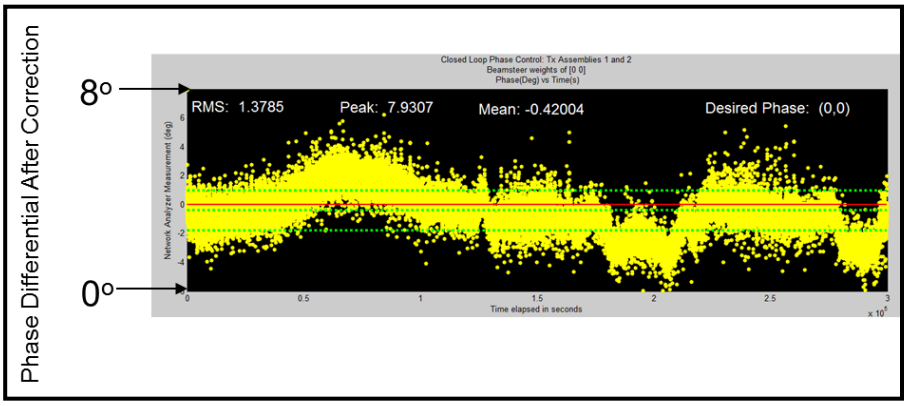


Fig 13 Phase transfer: Required: 4° RMS and 10° Peak; Achieved: 1.4° RMS and 8° Peak

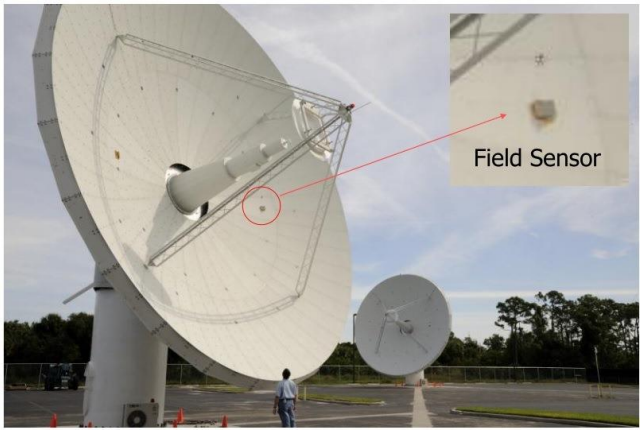


Fig 14 Left: Location of the circuit feedback sensor

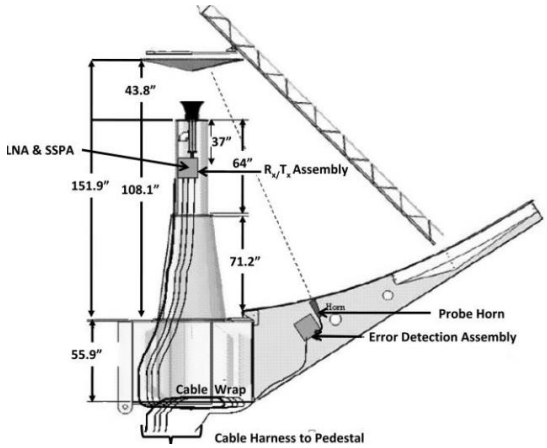


Right: Location of the error detection assembly

Fig 15 shows the phase changes before correction due to the circuitry heating and cooling during this 83+ hour test. Note the scale on the y-axis goes from 0 to 360°.

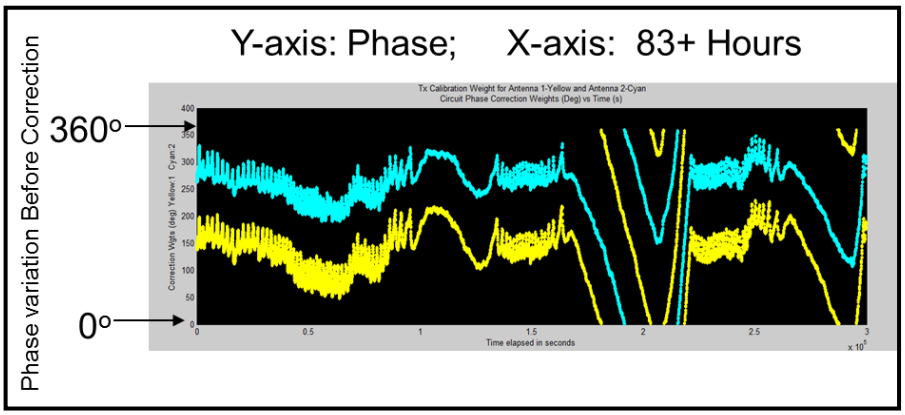


Fig 15 Phase changes due to circuitry before correction

The array transmitted at X band to DSCS B13. Downlink from B13 allowed performance observation but was not used for uplink beamforming. Fig 16 shows measured EIRP as sensed by B13. Almost ideal performance was realized, showing the $N^2$ effect as different antennas were turned off and on.

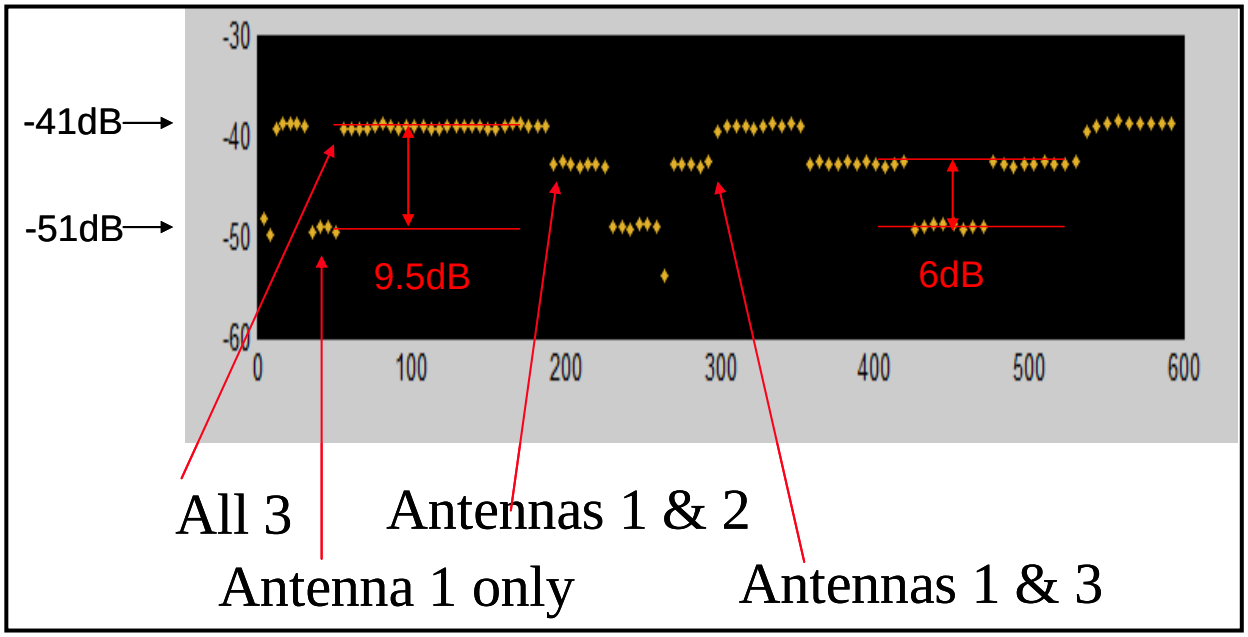


Fig 16 Measured uplink performance

*3.5.3 Real-time mitigation of tropospheric effects*

The third error contributor was phase variation due to the atmospheric. Even at X-band, tropospheric disturbances create signal path phase differentials between the antennas. Each reflector 'sees' a different column of atmosphere. Our method sensed and corrected phase variations due to the troposphere in real-time. A prerequisite was successful implementation of the continuous closed loop circuit technology and phase transfer on the receive path; with this correction being continually made any departure of the receive steering vector from the modeled can be interpreted as due to propagation variation. This phase variation is used to correct the modeled uplink phase settings. The receive and transmit targets can be anywhere within the element beam as shown in Fig 17.

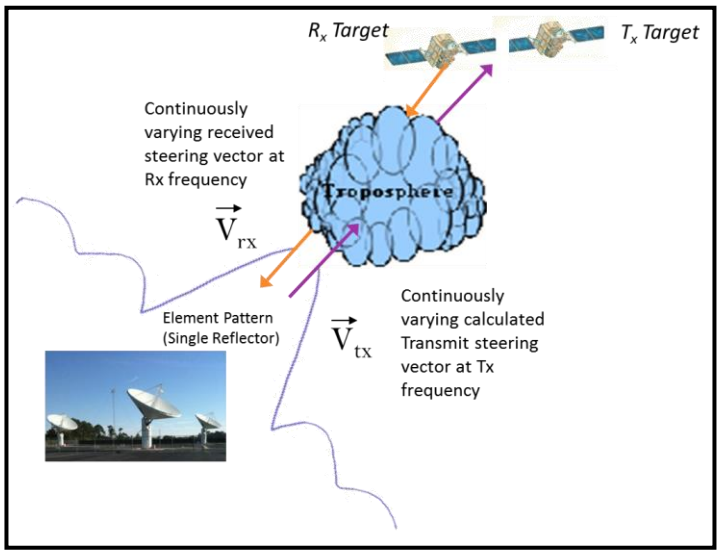


Fig 17 Real-time tropospheric variation mitigation

Details of the interesting period of time from about 100 to 450 s are provided in, Fig 18. The difference between measured received (measured) steering vector and modeled (top plot) are attributed to differential propagation effects. The middle plot depicts the single antenna received power measurement and the bottom depicts the optimized array output power measurement obtained from the demodulator. Tropospheric compensation (also called Instant Return) was OFF during the first part of this record and ON for the remainder. A vertical red line is drawn at the time of switch which occurred at about 310s. With atmospheric mitigation running errors were <0.3dB, without it running errors were ~2.2dB.

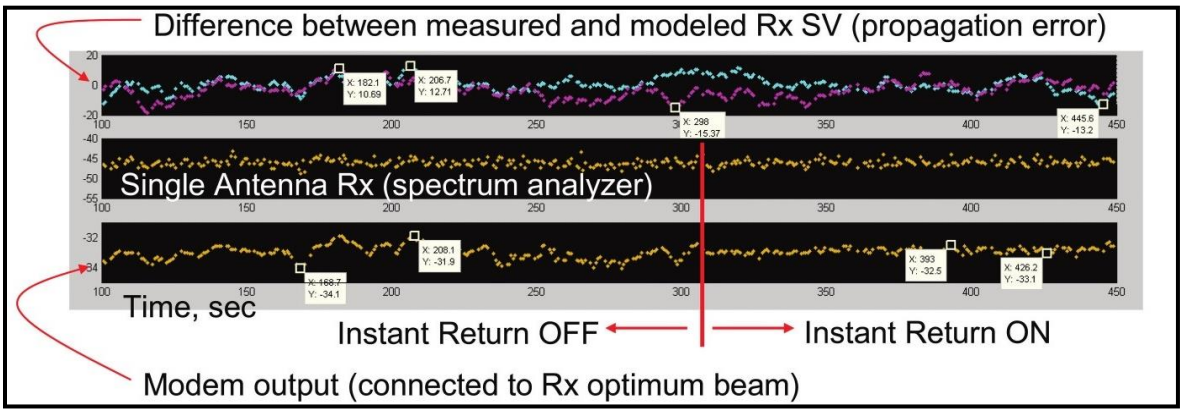


Fig 18 Coherent uplink arraying during a tropical depression

## 4. FUTURE DIRECTION

The widely-spaced Equatorial Space Situational Awareness Radar, ESSAR has the potential to comprehensively detect all persistent Earth-propagating objects; most in just months. It could complement Space Fence's ability to instantaneously detect objects flying through its field of view. ESSAR's performance characteristics include 24/7 availability, low system cost and complexity and the ability to see objects missed by other systems.

The enabling technologies include its unique location and orientation, on or near the Equator pointing towards the horizon, our previously demonstrated coherent transmit arraying technology [3], very high accuracy AOA and specialized hardware and algorithms. Together they make one-pass accurate object characterization possible. For example low altitude marble-sized objects could be accurately characterized with only three 12m ground reflectors.

The array is expandable to more or different sized antenna elements and/or larger HPA's. With performance having $N^3$ dependence, inverse fourth power radar range dependence can be significantly mitigated by adding elements to the array. This could facilitate effective detection and characterization of HEO objects (orbit, ISAR image) with only a modest elevation plane scan.

ESSAR could be a low-cost enhancement to the U.S. Space Surveillance Network and detections and orbital elements incorporated into database for asset protection and space situational awareness. After additional simulations and performance analysis, the system could be built and tested locally before relocation to a site such as Ecuador. During the first phase the specialized hardware could be built and tested while the specialized algorithms were being developed to run the operational system.

## 5. REFERENCES

1. U.S. Utility Patent 9,989,634,System and method for detection and orbit determination of Earth orbiting objects, Specialized Arrays Inc., 2018

2. Reality Check team (2018, August 17). Reality Check: Why is President Trump creating a space force? Retrieved from https://www.bbc.com/news/world-us-canada-45171311

3. Martin G.P. and Minear, K. et al, Large Reflector Uplink Arraying, *AIAA*, Reston, Virginia, "Space Operations Exploration, Scientific Utilization, and Technology Development, Vol. 235, Ch. 24, 409-228, 2011.

4. Martin G.P. and Minear, K. et al, "Large Reflector Uplink Arraying", in Proceedings of AIAA SpaceOps 2010 Conference, Huntsville, Alabama, April 2010

5. Davarian,F., IEEE, Uplink Arraying for Solar System Radar and Radio Science, Vol. 99, 783-793, May 2011.

6. Goddard Space Flight Center (2012, March 13). NASA GSFC Solicitation: High Power Uplink (Near Earth Objects Characterization. Retrieved from http://www.spaceref.com/news/viewsr.html?pid=40275

7. NASA HQ (2012, March 13). A—High Power Uplink Solicitation Number: NNH12429421R https://www.fbo.gov/?s=opportunity&mode=form&id=c5066f41a045db5a167db138306794d6&tab=core&_cview=0

8. U.S. Utility Patent Application Serial No. 15/013,283 System and method for widely-spaced coherent transmit arraying using a remote receiver